Metrol. Meas. Syst., Vol. 31 (2024) No. 3, pp. 595–608
DOI: 10.24425/mms.2024.150284

PAN POLSKA AKADEMIA NAUK

METROLOGY AND MEASUREMENT SYSTEMS
Index 330930, ISSN 0860-8229
www.metrology.wat.edu.pl

M&MS

EFFECT OF TM^{3+} ION DOPING ON THE POSSIBILITY OF BRAGG RESONATOR INSCRIPTION USING AN EXCIMER LASER

Krzysztof Skorupski[1)], Piotr Miluski[2)], Damian Harasim[1)], Jacek Klimek[1)], Patryk Panas[1)], Piotr Kisała[1)]

1) Lublin University of Technology, Nadbystrzycka 38A, 20-618 Lublin, Poland (✉ *p.kisala@pollub.pl*)
2) Faculty of Electrical Engineering, Bialystok University of Technology, 45D Wiejska Street, 15-351, Bialystok, Poland

Abstract

In this study, a comprehensive analysis of the lanthanide doping effect on the possibility of producing Bragg resonators using a UV excimer laser is presented. To fabricate the optical fibre preform, modified chemical vapour deposition (MCVD) technology equipped with a doping system using organometallic lanthanide compounds produced by Optocore was used. The efficiency of the fibre Bragg grating (FBG) inscription process was examined. Inscription of gratings was performed using manufactured fibre subjected and not subjected to hydrogen loading. The changes in three parameters characterizing the FBG spectra during exposure to the UV laser beam were determined. The efficiency of grating inscription on the produced lanthanide-doped fibres was compared to those on SMF-28 and NUFERN GF1 fibres. Since the spectral response is a key parameter determining the possibility of using FBGs for fibre laser construction, the temperature sensitivity for FBGs inscribed in the considered fibres was determined.

Keywords: MCVD, Bragg resonators, temperature sensitivity, fibre laser.

1. Introduction

Optical fibres doped with lanthanide compounds are commonly used in the construction of new polymeric sensors [1] and radiation sources, including lasers and sources with broadband emission [2–7]. Fibre lasers have attracted special attention due to their favourable operating parameters and the possibility of compact construction of laser and sensor systems [8,9]. Undoubted advantage resulting from the simple and closed construction of a resonator are system robustness and operational stability. In classic constructions of bulk lasers, the resonator system consists of mirrors that require precise alignment. A disadvantage of this type of construction is the possibility of contamination of the mirrors due to the open construction of the resonator, which can lead to damage of the resonator cavity and, consequently, of the entire system. In bulk systems, heat removal from the active medium is also a difficult task. In fibre lasers, due to favourable geometric conditions (a large side surface in relation to the volume of the active medium), it is

Article history: received January 11, 2024; revised March 25, 2024; accepted April 8, 2024; available online June 16, 2024.

much easier to meet the heat dissipation requirements. An additional advantage of fibre optic laser constructions is the ability to fabricate a resonator system inside the optical fibre using Bragg gratings. Commercially available Bragg gratings are produced by irradiation of passive optical fibres and are combined with active fibres using the electric arc welding technology [10]. An undoubted advantage would therefore be the possibility of directly fabricating Bragg resonators in optical fibres doped with rare earth elements (lanthanides), which would thus act as the active medium in the structure of the laser system. It is possible to design and manufacture fibres that can be spliced with photosensitive fibres with FBGs inscribed. However, the differences in the dimensions of the fibre core between photosensitive fibres (e.g., NUFERN GF1) and lanthanide-doped fibres can lead to unexpected interference, which will be observed in the spectra. Splicing should also be performed using precisely measured lengths of fibre sections. These inconveniences could affect the efficiency of laser generation in the proposed applications. The technology of fabricating Bragg mirrors using a phase mask and UV laser radiation is based on spatial modification of the refractive index in the area of the optical fibre core. Due to the significant power densities that can be obtained in the ultraviolet range using the 4th harmonic of a Nd-YAG laser with a radiation wavelength of 266 nm, polymer optical fibres made of *polymethyl methacrylate* (PMMA) can be utilized for this fabrication [11]. The *photosensitivity of the polymer* (PMMA) may be increased through the use of dopants such as benzyl dimethyl ketal or trans-4-stilbene methanol [12]. In the case of the construction of silica optical fibres, an excimer UV laser operating at a wavelength of 248 nm is most often used [13]. Photosensitivity of the fibre is obtained in this case by doping the core with *germanium dioxide* (GeO_2) at a level of 3% or higher. This provides the possibility of modifying the refractive index at the level of 10–4 [14]. A fibre Bragg grating inscription process with good reproducibility has been shown for single-mode Tm3+ fibres using the solution doping MCVD technology developed by the group of Prof. Ivan Kasik. Additionally, a monolithic fibre Tm3+ laser at 1951 nm and the wavelength shift vs. the generated power (1.41 pm/mW) were reported [15]. In the article, FBG gratings were inscribed directly in an active fibre doped with Tm3+ ions, without the germanium oxide dopant. The wide possibilities for fibre Bragg grating construction (number of fringes, period, modulation depth, inclination of fringes and tilt angle [16, 17]) provide numerous possibilities for spectral reflectance profile modification. Moreover, the possibility of using gratings with a variable period additionally expands the performances of gratings with a wide spectrum (*full width at half maximum* (FWHM) on the order of 1–3 nm), which is particularly advantageous in the construction of fibre lasers.

2. Methodology

Modified chemical vapour deposition (MCVD) technology equipped with a doping system using organometallic lanthanide compounds (chelate doping technology) produced by Optocore was used to fabricate the optical fibre preform. $Tm(tmhd)_3$ and Al_2O_3 complexes with helium carrier gas were used for doping the preform with Tm^{3+} ions. Oxygen lines were used to deliver silicon tetrachloride ($SiCl_4$) and germanium tetrachloride ($GeCl_4$) to an ultrapure Heraeus F300 tube (28/24 mm outer/inner diameter). A closed-loop automatic control system incorporating a pyrometer, a burner, and mass flow controllers was used to regulate the deposition rates and hot zone parameters. The refractive index profile was measured (He-Ne, 632.8 nm) using a P104 preform analyser. The single-mode structure of the optical fibre was designed with a core of 10 μm and a standard cladding diameter of 125 μm, which is desirable for easy splicing with commercial optical fibres. An additional polymer cladding, with a refractive index of 1.375 (UV-cured), was used to increase the mechanical durability of the fibre. A control interface drawing tower with

Metrol. Meas. Syst., Vol. 31 (2024), No. 3, pp. 595–608
DOI: 10.24425/mms.2024.150284

a Centorr furnace set at 2030°C was used for fibre drawing. The estimated (based on the refractive index delta) GeO_2 and Tm_2O_3 concentrations were 5.3 and 0.5 wt.%, respectively. Then, optical Bragg gratings were written in these optical fibres using the phase mask technology. For this purpose, an excimer laser (Coherent Bragg Star M) operating at a wavelength of 248 nm was used. The laser system provides a repetition rate of up to 100 Hz for fast grating inscription. The phase mask (Ibsen Photonics) assembly was illuminated by a large and static beam covering the entire FBG area of 10 mm in length. Due to the required large field size, a high-coherence excimer laser with up to a 100 mJ pulse energy was used for the static beam approach. A 10-millimetre section of the optical fibre was exposed to UV radiation. The inscription process was carried out using optical fibres previously subjected to a hydrogen-loading process and a fibre without hydrogenation. The hydrogen diffusion process was carried out at a pressure of 160 MPa and a temperature of 22°C for 14 days. The grating inscription process was performed with a pulse energy of 78 mJ and a repetition rate of 50 Hz. By hydrogenating the fibre for 14 days, we ensured that the hydrogen concentration in the fibre core was high, and its value was over 95%. With a shorter hydrogenation time, the efficiency of Bragg grating inscription is lower because the hydrogen concentration in the fibre core is lower and the structure recording becomes more difficult. The hydrogen saturation depends on the temperature and pressure. The hydrogenation time can be shortened by increasing the pressure the hydrogenated fibre is subjected to in the hydrogen atmosphere, as well as by increasing the hydrogenation temperature.

3. Results

The measured refractive index profile of the preform is presented in Fig. 1a. The core/cladding NA was estimated to be 0.244 based on the Δnc.a. $14 \cdot 10^{-3}$. The fibre dimensions were measured using an optical microscope, and the core/cladding ratio was 10/125 µm. A photo of the fibre is presented in Fig. 1b.

The fibre shown in Fig. 1 was then subjected to the Bragg structure inscription process. To verify the possibility of accelerating the production of this type of structure, fibre hydrogenation tests were also performed. Section 3.1 summarizes the results of spectral measurements of structures not subjected to the hydrogenation process. Section 3.2 presents analogous measurements, but for the case when the fibres were subjected to the photosensitization process by hydrogenation.

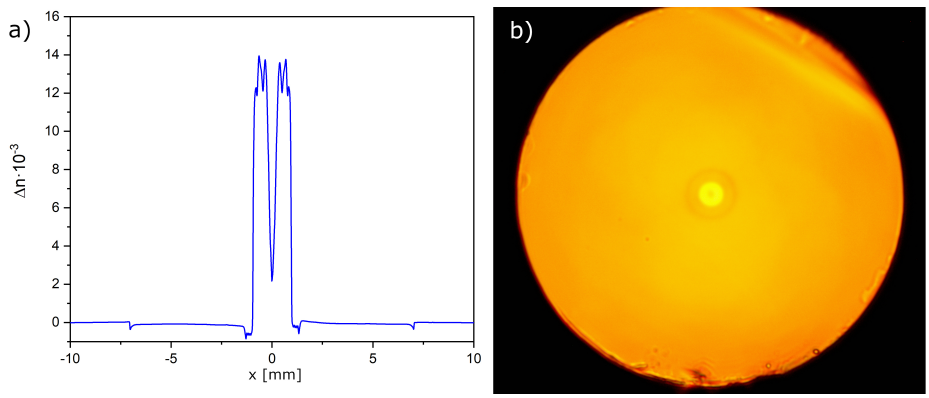

Fig. 1. Refractive index profile of the fabricated preform •10^{-3} (a), and cross-section of a Tm-doped fibre (b).

3.1. Bragg mirror inscription in nonhydrogenated Tm3+ ion-doped fibres

The first experimental measurements concerned the possibility of inscription of FBGs with the highest possible reflectance in nonhydrogenated fibres. The experimental system was set up to constantly control the UV-light inscription process. To monitor the spectral parameters of the inscribed gratings, a Yokogawa AQ6370D optical spectrum analyser and a Thorlabs S5FC1550S broadband light source were used. The measurement setup provided the possibility of measuring the transmission spectra. The laser pulses were continuously started, and the spectra were measured with a 1 second time interval. Note that a single measurement using an OSA required a fraction of a second to be performed. The applied time interval resulted in the effect that the left side of the spectral characteristics, corresponding to shorter wavelengths, was measured at a different time than the right side, corresponding to longer wavelengths. This was intentional because in this part of the work, the aim was to investigate the trend of the changes in the shape and position of the spectral characteristics and, above all, the possibility of producing Bragg mirrors directly in optical fibres doped with rare earth elements. The measurement results are summarized in Fig. 2. This figure includes the spectral characteristics of the unmodified fibre (Inset 1) and the spectral characteristics measured at the end of the inscription process (Inset 2). Measured as a function of time, the direction of the changes in the shape of the spectral component corresponding to the Bragg resonance is marked with an arrow.

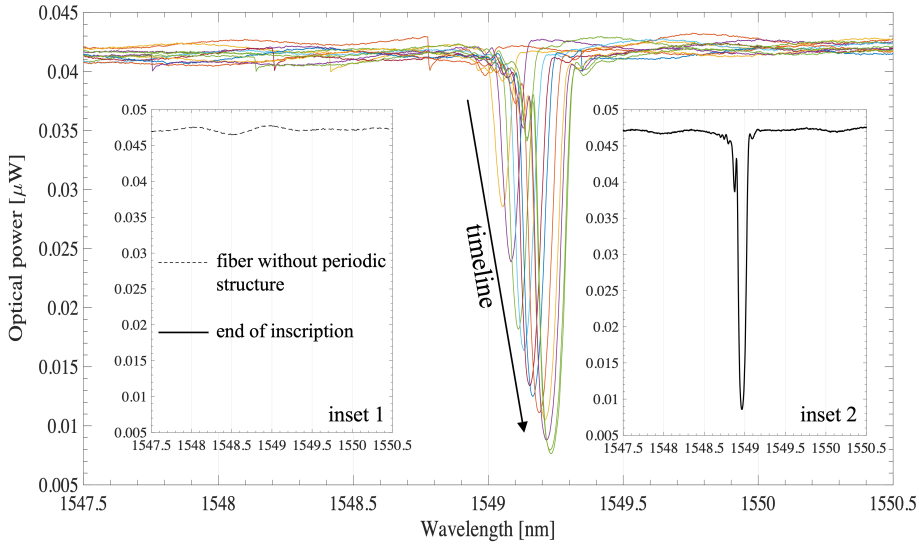

Fig. 2. Evolution of the transmission spectrum during the FBG inscription process.

As shown, exposing the fibre to UV light at 248 nm increases the reflection (amplitude) of the core Bragg mode dip in the transmission spectrum. There is also an observable shift towards longer wavelengths. This shift is related to the increase in the effective refractive index within the inscribed Bragg structure. Analysis of the distribution of the refractive index in the Bragg grating shows two components of the refractive index variation related to the FBG manufacturing process. One is the variable component Δn_{AC} related to the depth of the index change in the created periodic zones, and the other is the constant component Δn_{DC} resulting from the imperfections of this process. Because of the use of the phase mask method, the constant component is mainly caused by the propagation of light in the form of zero-order diffraction. While maintaining a constant

value of the grating period Λ, both components Δn cause an increase in the average value of the effective refractive index n_{eff} and a shift in the central Bragg length λ_B towards longer wavelengths according to the following equation:

$$\lambda_B = 2\pi n_{\text{eff}} \Lambda. \tag{1}$$

During the FBG inscription process, a gradual shift of the spectra is observed, which is known as the redshift.

The shift phenomenon is more clearly visible if we only present selected spectral characteristics. Figure 3 shows the spectral characteristics measured at specific times during the manufacturing of the gratings.

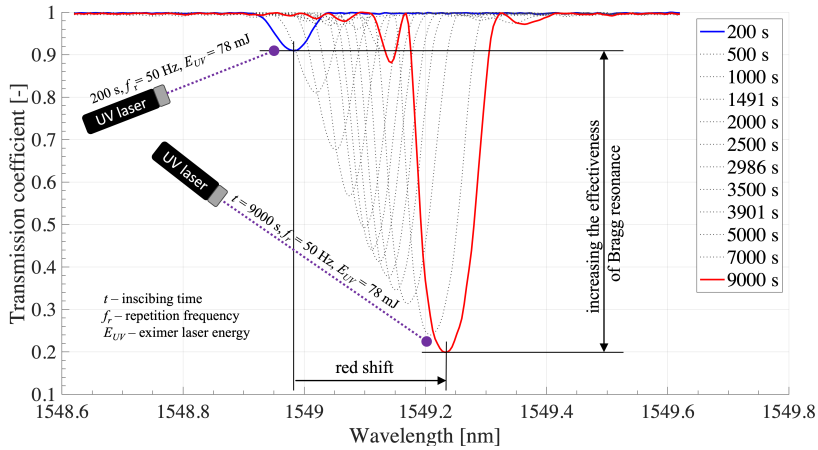

Fig. 3. Evolution of the FBG transmission spectrum measured for defined timestamps during pulse laser inscription.

The selected timestamps marked in Fig. 3 were used to determine the points at which the key parameters of the manufactured structures were distinguished. These key parameters are primarily the Bragg wavelength, the *full width at half maximum* (FWHM) and the normalized transmission coefficient determined for the Bragg wavelength. Figure 4 shows a summary of these three key parameters. With increasing exposure time of the doped fibre to the UV interference pattern, the entire spectral characteristics presents a redshift (Fig. 3). This, in turn, results in a shift in the Bragg wavelength (Fig. 4a), i.e., an increase in the resonance wavelength. This change is monotonic over the entire range of changes during the exposure time of the structures, which proves that there is no so-called saturation of the structure inscription. At the same time, there is also a noticeable increase in the FWHM (Fig. 4b) of the FBG main transmission peak, which, in turn, is related to the enlargement (proportional increases in width and height) of the spectral characteristics. An interesting phenomenon is also the formation of nonmonotonic regions in the FWHM = $f(t)$ characteristics. This is most likely related to the method of determining the FWHM parameter, which is determined as half the height of the main transmission peak. It is also possible to use a high-precision demodulation method based on the amplitude ratio curve instead of the FBG reflection spectrum, which can significantly increase the sensing precision [18]. Due to the existence of the so-called side lobes in the spectral characteristics and the irregular shape of the transmission dip, determining its half-width is not always simple and effective. This does not change the fact that the general trend of the FWHM parameter during the entire structure recording process is as shown in Fig. 4b, in which this parameter reaches a higher value for longer exposure times of the doped fibre to UV light.

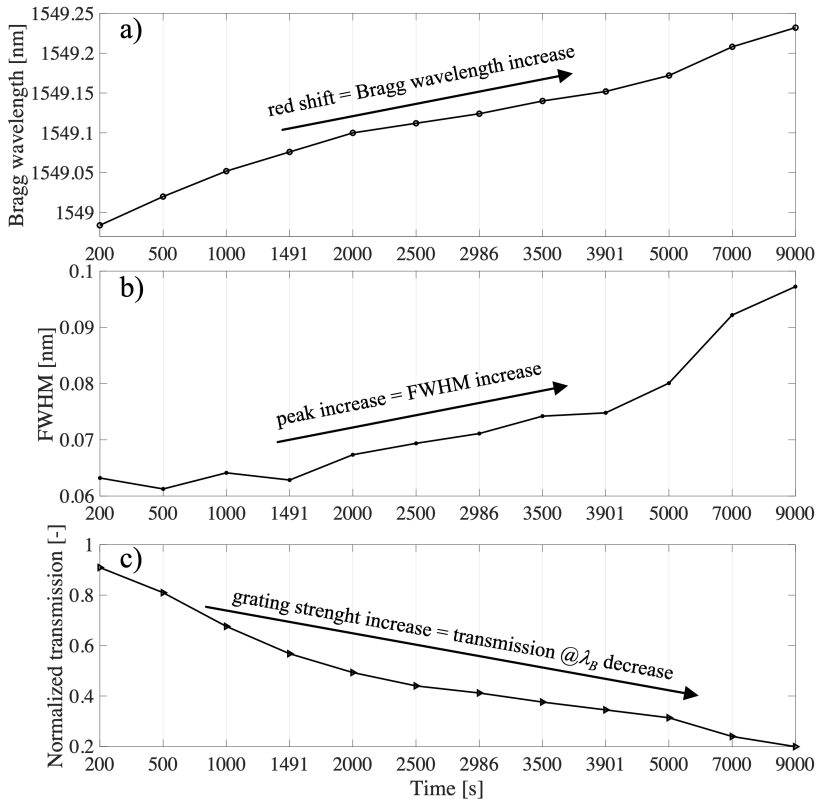

Fig. 4. Changes in the key parameters of the inscribed structures over time: Bragg wavelength (a), full width at half maximum (b) and normalized transmission coefficient determined for the Bragg wavelength.

Another tendency can be observed for the normalized transmission coefficient determined for the Bragg wavelength λ_B (Fig. 4c). As the exposure time of the fibre to UV light increases, so does the accumulated energy delivered to the illuminated section of the fibre, which causes an increase in the reflection of the grating [19]. The increase in the grating "strength" is, in turn, manifested by an increase in the reflection of wavelengths in the range close to the Bragg wavelength. This increases the reflectivity of the structure, which is directly transformed into a decrease in its transmittance for the wavelength corresponding to the Bragg resonance according to (1). All the described effects presented in this section are for doped fibres that were not hydrogenated. Section 3.2 presents similar results but with the additional technological procedure of diffusing hydrogen in the doped structures.

3.2. Bragg mirror inscription in hydrogen-loaded Tm^{3+} ion-doped fibres

The results presented in Section 3.1 concerned doped fibres not subjected to additional photosensitization treatments. In the following section, we present the results of manufacturing structures that have been subjected to hydrogen loading to increase their photosensitivity. First, the susceptibility of the doped fibres to the hydrogenation process itself was examined. This procedure was carried out in accordance with the procedure described in Section 2. The process

was carried out at a pressure of 160 MPa and a temperature of 22°C for 14 days. These conditions were controlled and kept stable throughout the hydrogen loading process. After this process was completed, the Bragg grating inscription was begun, during which the spectral characteristics were constantly monitored. These characteristics, similar to those in the case of nonhydrogenated fibres, were measured in the transmission mode and are summarized in Fig. 5.

Comparing the characteristics collected during the production of nonhydrogenated (Fig. 3) and hydrogen-loaded (Fig. 5) structures, differences in the key parameters of the structures are visible. First, the FBG writing process is significantly accelerated as a result of the hydrogenation of the fibres. The fact that the fibres can be photosensitized through hydrogenation is a great advantage. Second, we see a significant improvement in the key parameters of the structures. For example, the normalized transmission coefficient for nonhydrogenated fibres reaches the minimum value $t = 0.2$ for the Bragg wavelength (λ_B) after $T = 9000$ s. However, the normalized transmission coefficient of hydrogenated fibres reaches the minimum value (for λ_B) of $t = 0.075$ after $T = 550$ s. There is also a large difference in the redshifts during the inscription process. In the case of nonhydrogenated fibres, the redshift $\Delta\lambda$ is 0.25 nm (after 9000 s). For fibres subjected to hydrogen loading, the redshift rate increases, and reaches 0.4 nm after only 550 s. In conclusion, it should be stated that the hydrogen loading process significantly increases the dynamics of manufacturing structures in such prepared doped fibres.

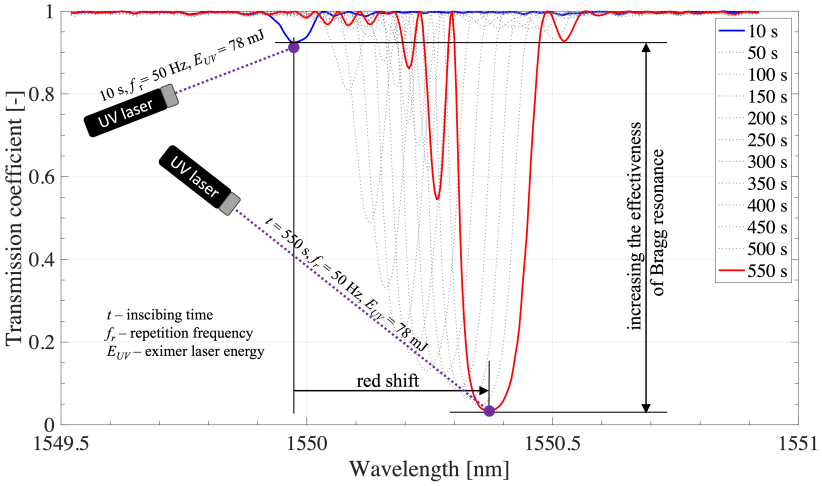

Fig. 5. Transmission spectra measured during the Bragg structure inscription process after hydrogenation.

Figure 6 summarizes the three key parameters of hydrogenated fibres. As we can see, as the exposure time of the doped fibre to the UV laser beam increases, a shift in the Bragg wavelength (Fig. 6a) towards longer wavelengths is visible, as in the case of nonhydrogenated fibres.

The change in the central wavelength is monotonic over the entire range of changes during the structure exposure time. There is also a noticeable increase in the FWHM (Fig. 6b) of the main transmission dip in the structure spectrum, which, similar to the case of nondoped nonhydrogenated fibres, is related to the enlargement of the main transmission dip. Additionally, as in the case of nonhydrogenated fibres, for the full width at half maximum, a nonmonotonic region appears at the very beginning of the inscription of the structures. This phenomenon is explained in Section 3.1. The trend of the FWHM during the entire FBG inscription process is shown in Fig. 6b. The spectral width increases, reaching a higher value at longer exposure times of the doped fibre to UV light.

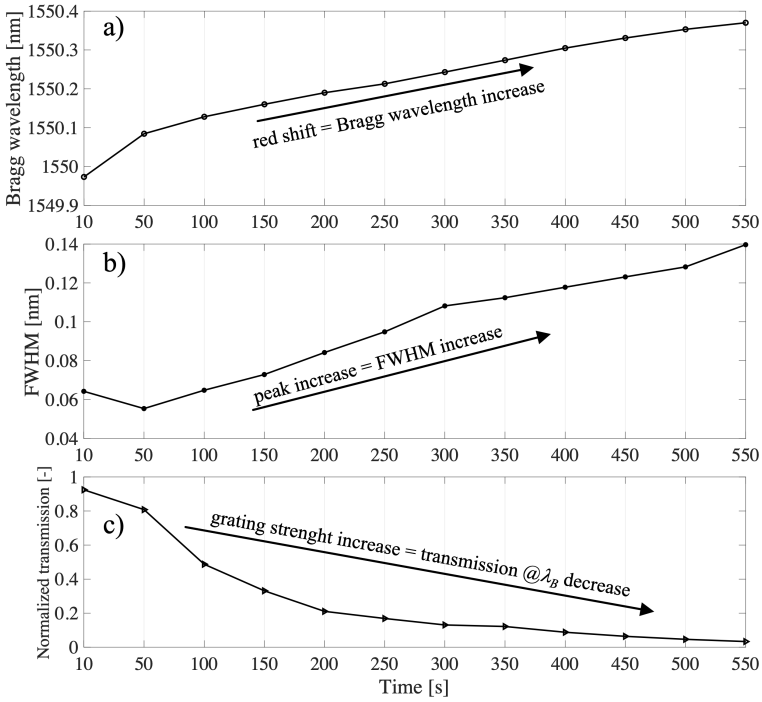

Fig. 6. Changes in the key parameters of the inscribed structures over time: Bragg wavelength (a), full width at half maximum (b) and normalized transmission coefficient determined for the Bragg wavelength.

As in the case of nonhydrogenated fibres, the opposite tendency for the normalized transmission coefficient determined for the Bragg wavelength $\Delta\lambda_B$ can also be observed in this case (Fig. 6c). The transmission coefficient corresponding to the resonance wavelength of the produced structures decreases with increasing excimer laser exposure time. The feedback of modes in the grating becomes increasingly effective, the reflection coefficient increases, and consequently, the transmission coefficient of the mirror decreases. To determine the effect of Tm^{3+} ion doping on the possibility of Bragg resonator inscription using an excimer laser, we also attempted to record resonators in ordinary, standard SMF-28 fibres. We compare all the key parameters and present the results in Section 3.3.

3.3. Measurements of the parameters of Bragg mirrors in fibres doped with thulium ions and SMF-28 fibres

In Sections 3.1 and 3.2, we presented the possibility of manufacturing Bragg gratings in fibres doped with Tm^{3+} ions. We have shown that hydrogen loading of these fibres significantly accelerates the dynamics of the FBG inscription process. We have proven that these fibres are perfect materials in which laser mirrors can be directly manufactured without the need to weld (insert into the fibre optic line) other fibres, e.g., photosensitive fibres. In this section, we compared the key parameters of gratings manufactured in SMF-28 fibres, fibres doped with thulium ions and fibres doped with thulium ions and treated by a hydrogen-loading process. Fig. 7 summarizes the changes in all the key parameters of the manufactured structures over time.

Metrol. Meas. Syst., Vol. 31 (2024), No. 3, pp. 595–608
DOI: 10.24425/mms.2024.150284

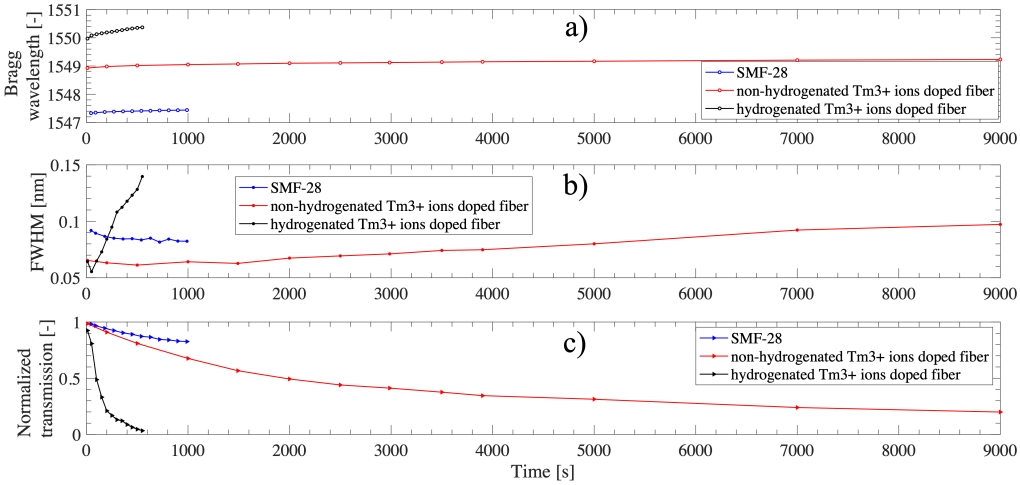

Fig. 7. Comparison of key parameters of inscribed structures over time: Bragg wavelength (a), FWHM (b) and normalized transmission coefficient determined for the Bragg wavelength.

The measurement results presented in Fig. 7 illustrate the effect of Tm^{3+} ion doping on the possibility of Bragg resonator inscription using an excimer laser. As we can see, it is possible to inscribe Bragg structures in lanthanide-doped fibres even without their prior hydrogenation. A comparison of the characteristics in Fig. 7 (red and blue curves) reveals that the changes in the FWHM, Bragg wavelength and normalized transmission are similar. The doped fibre allows FBG recording, and only a longer exposure time to laser light is required. A significant increase in the dynamics of the Bragg structure recording is observed after Tm^{3+}-doped fibre hydrogenation, as shown in Fig. 7 (black curve). Extinction of fibre transmission at the Bragg wavelength is extremely important in the construction of laser mirrors. It determines the effectiveness of a given mirror. As we can see from Fig. 7c, the reduction in the transmission coefficient is the fastest and most effective in the case of a thulium ion-doped and simultaneously hydrogenated fibre.

4. Temperature sensitivity of Bragg mirrors inscribed in Tm^{3+}-doped fibres

Analysis of the spectral response of inscribed mirrors to temperature changes is key to determining the possibility of their application in laser generation. It is also important in the case of other possible applications, as the FBG mirror inscribed in a conventional fibre could be used as an optical filter. For this purpose, the spectral shifts of FBGs inscribed in three types of hydrogen-loaded fibres were investigated: a Tm-doped fibre, a GF1 (Ge-doped) photosensitive NUFERN fibre and an SMF-28 fibre. All the characteristics were measured at a proper time after the hydrogen-loading process and grating inscription to ensure that all the additional H_2 molecules had left the fibre structure. Placing the fibre at an elevated temperature can increase the speed of the process of hydrogen atoms leaving the fibre structure. The waiting time was determined based on experimental tests involving cyclic measurements of the spectral characteristics of gratings placed in a climatic chamber at a high temperature. The process of hydrogen molecules leaving the fibre was considered complete when the changes in the FBG spectra during measurements of the heated fibre stopped. For our measurements, hydrogen-loaded fibres with FBGs inscribed were placed at 80°C for 14 days.

A thermal chamber was used to maintain a stable temperature while the FBG spectra were measured using an optical spectrum analyser. In a real experiment, three fibres with gratings inscribed were placed at the same time in the chamber to provide the same conditions for every measured spectrum. Fig. 8 shows the characteristics of three FBGs inscribed in Tm-doped fibres with different grating periods and different depths of index modulation measured at temperatures of 0°C, 40°C, 80°C and 120°C.

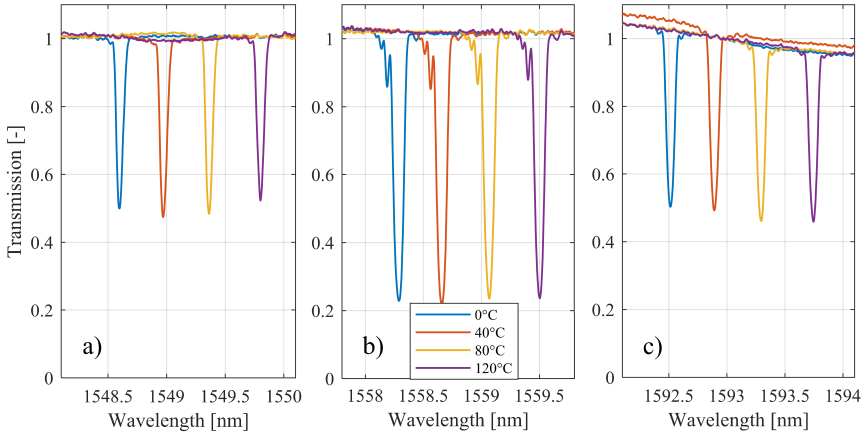

Fig. 8. Transmission spectra of FBGs inscribed in Tm-doped fibres with different reflectivities and grating periods: a) 1069,24 nm; b) 1075,86 nm; c) 1100 nm.

An increase in the ambient temperature results in a shift of the grating central wavelength, which is typical. Moreover, the shape and FWHM of the spectra do not change. The experimentally determined average sensitivity of gratings inscribed in Tm-doped fibres is 0.10321 nm/°C. The wavelength shift in response to temperature changes of the 3 FBGs inscribed with different grating periods is presented in Fig. 9.

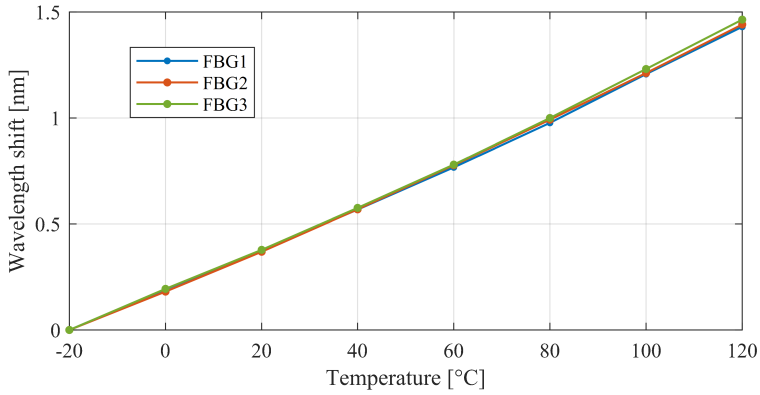

Fig. 9. Wavelength shift of FBGs inscribed in Tm-doped fibres caused by ambient temperature changes from −20 to 120 °C.

The temperature sensitivity of the FBGs in Tm-doped fibres is similar to the sensitivities obtained for gratings inscribed in hydrogen-loaded commercially available SMF-28 and GF1 fibres. A direct comparison of the characteristics of the wavelength shift in response to temperature

changes for the FBGs inscribed in different types of fibres is presented in Fig. 10. The sensitivity of the FBG inscribed in the new Tm-doped fibre is slightly greater than that in the other cases. The linearity of the shift is maintained over the whole measured temperature range.

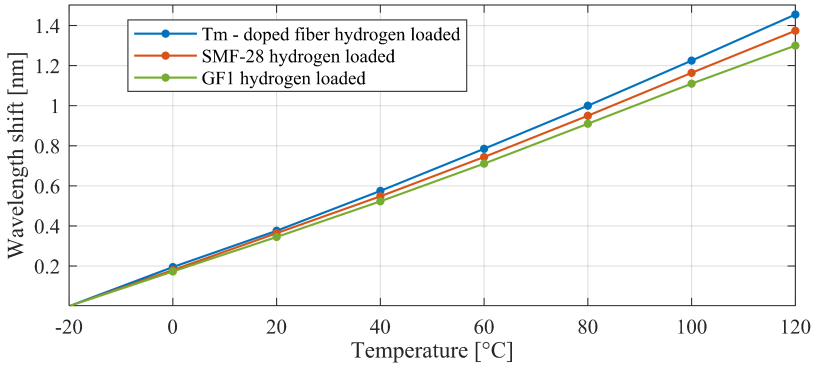

Fig. 10. Characteristics of the wavelength shift in response to temperature changes for FBGs inscribed in the three considered fibre types.

The sensitivities obtained from the measurements and presented characteristics are shown in Table 1.

Table 1. Sensitivities of the wavelength shift in response to temperature changes of FBGs in different fibres.

Fibre	Sensitivity [pm/K]
Tm-doped	0.10321
SMF-28	0.09814
GF1	0.09286

The results show that the sensitivities of the wavelength shift in response to temperature changes are similar for the FBGs manufactured in the designed Tm-doped, SMF-28 and GF1 fibres. In every case, changes in the ambient temperature do not affect the shape or FWHM of the spectra. This leads to the conclusion that the gratings inscribed in these types of optical fibres could be used in the same measurement system as sensors and band gap filters.

5. Conclusions

In this article, we presented the possibility of producing laser mirrors in lanthanide-doped fibres. An important goal of this research was to prove that such fibres are susceptible to the hydrogenation process. This process is very effective and significantly increases the dynamics of inscribing FBG structures. Bragg mirrors were inscribed in lanthanide-doped fibres using a 248 nm excimer laser and characterized. We demonstrated significant improvements in the key parameters of such FBG structures. The normalized transmission coefficient for nonhydrogenated fibres reaches 0.2 for the Bragg wavelength after 9000 seconds. However, the normalized transmission coefficient of hydrogenated fibres reaches 0.075 after 550 s. We also demonstrated a difference in the redshifts during the inscription process. In the case of nonhydrogenated fibres, the redshift $\Delta\lambda$ is 0.25 nm after 9000 s. For fibres subjected to hydrogen loading, the redshift rate increases, and

the redshift reaches 0.4 nm after only 550 s. Additionally, an analysis of the spectral response of the inscribed mirrors to temperature changes is presented. This is one of the key factors determining the possibility of their application in laser generation. The obtained results prove the capability of using the presented mirrors in a wide range of applications.

Acknowledgements

The research leading to these results has received funding from the commissioned task entitled "VIA CARPATIA Universities of Technology Network named after the President of the Republic of Poland Lech Kaczyński", contract no. MEiN/2022/DPI/2575 action entitled "In the Neighbourhood – Inter-university Research Internships and Study Visits".

References

[1] Miluski, P., Kochanowicz, M., Żmojda, J., & Dorosz, D. (2016). UV radiation detection using optical sensor based on Eu3+ doped PMMA. *Metrology and Measurement Systems*, *23*(4), 615–621. https://doi.org/10.1515/mms-2016-0049

[2] Hasegawa, Y., & Nakanishi, T. (2015). Luminescent lanthanide coordination polymers for photonic applications. *RSC Advances*, *1*, 338–353. https://doi.org/10.1039/c4ra09255d

[3] Honzatko, P., Baravets, Y., Kasik, I., & Podrazky, O. (2014). Wideband thulium-holmium-doped fiber source with combined forward and backward amplified spontaneous emission at 1600-2300 nm spectral band. *Optics Letters*, *39*, 3650–3563. https://doi.org/10.1364/OL.39.003650

[4] Schuster, K., Unger, S., Aichele, C., Lindner, F., Grimm, S., Litzkendorf, D., Kobelke, J., Bierlich, J., & Wondraczek, K. (2014). Bartelt, H. Material and Technology Trends in Fiber Optics. *Advanced Optical Technologies*, *3*, 447–468. https://doi.org/10.1515/aot-2014-0010

[5] Miluski, P., Markowski, K., Kochanowicz, M., Łodziński, M., Żmojda, J., Pisarski, W. A., Pisarska, J., Kuwik, M., Leśniak, M., Dorosz, D., Ragiń T., Askirka V., & Dorosz J. (2023). Tm3+/Ho3+ Profiled Co-Doped Core Area Optical Fiber for Emission in the Range of 1.6–2.1 μm. *Scientific Reports*, *13*, 1–7. https://doi.org/10.1038/s41598-023-41097-2

[6] Michalska, M., Grześ, P., & Świderski, J. (2019). High power, 100 W-class, thulium-doped all-fiber lasers. *Photonics Letters of Poland*, *11*, 109–111. https://doi.org/10.4302/plp.v11i4.953

[7] Michalska, M., Honzatko, P., Grzes, P., Kamradek, M., Podrazky, O., Kasik, I., & Swiderski, J. (2023). Thulium-doped 1940- and 2034-nm fiber amplifiers: Towards highly efficient, high-power all-fiber laser systems. *Journal of Lightwave Technology*, *42*(1), 339–346. https://doi.org/10.1109/JLT.2023.3301397

[8] Prokopiuk, A., Bielecki, Z., & Wojtas, J. (2021). Improving the accuracy of the NDIR-based CO 2 sensor for breath analysis. *Metrology and Measurement Systems*, *28*(4), 803812. https://doi.org/10.24425/mms.2021.138578

[9] Bielecki, Z., Stacewicz, T., Wojtas, J., Mikołajczyk, J., Szabra, D., & Prokopiuk, A. (2018). Selected optoelectronic sensors in medical applications. *Opto-Electronics Review*, *26*(2), 122133. https://doi.org/10.1016/j.opelre.2018.02.007

[10] Yablon, Andrew D. (2005). *Optical Fiber Fusion Splicing*, Springer. https://doi.org/10.1007/b137759

[11] Pereira, L., Min, R., Hu, X., Caucheteur, C., Bang, O., Ortega, B., Marques, C., Antunes, P., & Pinto, J. L. (2018). Polymer optical fiber Bragg grating inscription with a single Nd:YAG laser pulse. *Optics Express*, *26*, 18096–18104. https://doi.org/10.1364/OE.26.018096

[12] Min, R., Pereira, L., Paixão, T., Woyessa, G., André, P., Bang, O., Antunes, P., Pinto, J., Li, Z., Ortega, B., & Marques, C. (2019). Inscription of Bragg gratings in undoped PMMA mPOF with Nd:YAG laser at 266 nm wavelength. *Optics Express*, *27*, 38039–38048. https://doi.org/10.1364/OE.27.038039

[13] Zhao, X., Tian, X., Wang, M., Rao, B., Li, H., Xi, X., & Wang, Z. (2021). Fabrication of 2 kW-level chirped and tilted fiber Bragg gratings and mitigating stimulated Raman scattering in long-distance delivery of high-power fiber laser. *Photonics*, *8*(9), 369. https://doi.org/10.3390/photonics8090369

[14] Archambault, J. L., Reekie, L., & Russell, P. St. J. (1993). 100% reflectivity Bragg reflectors produced in optical fibres by single excimer laser pulses. *Electronics Letters*, *29*(5), 453–455. https://doi.org/10.1049/el:19930303

[15] Peterka, P., Honzátko, P., Becker, M., Todorov, F., Písařík, M., Podrazký & O., Kašík I. (2013). Monolithic Tm-doped fiber laser at 1951 nm with deep-UV femtosecond-induced FBG pair. *IEEE Photonics Technology Letters*, *25*(16), 1623–1625. https://doi.org/10.1109/LPT.2013.2272880

[16] Kisała, P. (2022). Physical foundations determining spectral characteristics measured in Bragg gratings subjected to bending. *Metrology and Measurement Systems*, *29*(3), 573584. https://doi.org/10.24425/mms.2022.142275

[17] Kisała, P. (2023). Identification of cladding modes in SMF-28 fibers with TFBG structures. *Metrology and Measurement Systems*, *30*(3), 507–518. https://doi.org/10.24425/mms.2023.146418

[18] Zhang, X., Sun, F., Jiang, J., Feng, M., Wang, S., Fan, X., Yang, Y., & Liu, T. (2019). High-precision FBG demodulation using amplitude ratio curve with sharp peak. *Optical Fiber Technology*, *47*, 7–14. https://doi.org/10.1016/j.yofte.2018.11.020

[19] Mahakud, R., Prakash, O., Kumar, J., Nakhe, S. V., & Dixit, S. K. (2012). Analysis on the effect of UV beam intensity profile on the refractive index modulation in phase mask based fiber Bragg grating writing. *Optics Communications*, *285*(24), 5351–5358. https://doi.org/10.1016/j.optcom.2012.08.015

Krzysztof Skorupski received the M.Sc. degree in 2004 from Lublin University of Technology (LUT), Poland and Ph.D. from AGH University of Krakow in 2017. He is currently an assistant professor at LUT. His research interests are inscription and applications of fibre Bragg gratings.

Piotr Miluski received his Ph.D. degree (2010) in the field of metrology from Bialystok University of Technology and D.Sc. from Institute of Optoelectronics, Military University of Technology in Warsaw (2018). Since 2019 he has been an associate professor at Bialystok University of Technology. His research interests are applications of luminescent and functional materials and focused on glass and polymeric materials, luminescent optical fibres (fluorophores and rare-earths) and optical sensors.

Jacek Klimek received his Ph.D. from AGH University Krakow in 2021. He is an assistant professor at the Department of Electronics and Information Technology of Lublin University of Technology. His current research interests include the production and characterization of optical sensor systems based on complex Bragg grating structures.

Patryk Panas received the M.Sc. degree in Mechatronics in 2017 from the Faculty of Electrical Engineering and Computer Science of Lublin University of Technology (LUT). At the moment, he is employed as an assistant professor at the same university. He is involved in implementation of optical fibre sensors based on fibre Bragg gratings.

Damian Harasim has his received Ph.D. degree from the Faculty of Electrical Engineering and Computer Science at AGH University of Krakow, Poland in 2022. His current research interests lie in fabrication and characterisation of optical sensing systems, especially based on unconventional fibre Bragg grating structures. He is currently employed as an assistant professor at Lublin University of Technology, Poland.

Piotr Kisała received a diploma in informatics and computer networks from Maria Curie-Skłodowska University, Poland. He received the Ph.D. degree in 2009 and Habilitation degree in 2013 and the title of professor in 2020. He is currently head of Optoelectronic & ICT Department at LUT. His research interests include optical sensor projects, fabrication and testing and the design and development of unconventional FBG sensors. Prof. Kisała has authored over 80 journal publications and conference contributions and 6 patents.